

Supplementary Discussion

Note on observed B-factors.

RNA structures typically have much higher average B-factors than proteins. Reported B-factors for similar RNA crystal structures at a resolution comparable to those reported in this study include: FMN riboswitch, 5KX9 (98.9 Å²); PREQ1-II riboswitch, 5DDQ (69.5 Å²); SAM-I riboswitch, 5FK1 (116.4 Å²); and ligand-bound adenine riboswitch, 4TZX (46.1 Å²). Importantly the above mentioned crystal structures were determined under cryogenic conditions, and the temperature of data collection has a direct effect on observed B-factors. Moreover, the increased plasticity of small crystals used in SFX/XFEL experiments may result in higher B-factors as compared to those of structures determined from large, single crystals. Given that our reported structures are from micron size crystals of a flexible RNA molecule at room temperature, the observed average B-factors listed in Table 3 are in the expected range.

Additional noteworthy features of rA71 structures.

The kissing loop structures differ only in A64, which is in an *anti*-configuration in the apo structures, in contrast to a *syn*-conformation in the bound structure^{13,15}; A64 forms two hydrogen bonds with the Hoogsteen edge of A35 in both apo and IB conformers, whereas it forms only a weak hydrogen bond with A35 in the bound structure. Thus, the A35-A64 base pair may contribute to the stabilization of the kissing loops, in addition to the two known canonical G37•C61 and G38•C60 base pairs.

The destabilization of stem P1 in the apo and IB conformers is strongly indicated by incomplete electron density. The partially melted P1 was, at first, somewhat surprising because the version of the aptamer domain used for this study contains three consecutive G•C base pairs

at the end of P1. This suggests that the interactions and dynamics present in the ligand-free pocket are strong enough to partially override the intrinsic base-pairing potential of the P1 helix.

Multiphasic binding kinetics.

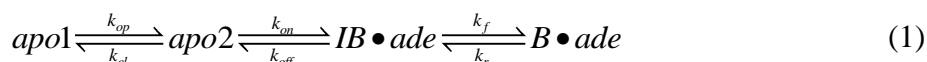
Early studies on purine riboswitches showed that ligand binding is slower than diffusion, pointing to a conformational change in the apo riboswitch that precedes ligand recognition^{14,57}. To ask whether both apo conformers contribute to ligand binding, we measured the adenine binding kinetics to apo-rA71 by replacing U48 with the fluorescent base-analog, 2-aminopurine (U482AP) (Extended Data Fig.4a). The multistage kinetics shows the presence of an intermediate bound (IB) state, in addition to slow exchange between binding incompetent and binding competent apo structures (Fig. 2c; Extended Data Fig. 4b,c). Simpler models that neglect these additional intermediate states could not describe the observed kinetics (Extended Data Fig. 4d,e); this is discussed below in further detail.

Adenine binding to the rA71-U482AP riboswitch in pseudo-first order conditions occurs in two observed kinetic phases: a fast phase that depends on ligand concentration, and a slow ligand-independent phase that becomes prominent above 50 μM adenine (Fig. 2d and Extended Data Fig. 4b). The slow, ligand-independent step suggests that part of the riboswitch population must undergo a conformational change before ligand binding, and this limits the rate of ligand sensing in high adenine concentrations (Extended Data Fig. 4b). The non-linear rise in the observed rate of the fast phase indicates at least one additional intermediate in the ligand-binding pathway (Extended Data Fig. 4b). At low adenine (0.5-25 μM), the increase in λ_{fast} with adenine concentration corresponds to an apparent bimolecular association rate constant $k_{\text{on}} = 1.9 \cdot 10^5 \text{ M}^{-1}\text{s}^{-1}$ in 10 mM MgCl_2 and $5.2 \cdot 10^4 \text{ M}^{-1}\text{s}^{-1}$ in 1.25 mM MgCl_2 (Extended Data Fig. 4c). These values are similar to the ligand binding kinetics of other purine riboswitches^{14,15,57} and

substantially slower than diffusion, indicating that some reorganization of the RNA structure is needed for ligand association^{14,58,59}. At adenine concentrations above 50 μM , the increase in 2AP fluorescence is limited by the rate of ligand-dependent reorganization of the riboswitch binding pocket, and the apparent k_{on} for adenine in 10 mM MgCl_2 begins to fall below $1.9 \cdot 10^5 \text{ M}^{-1}\text{s}^{-1}$.

Global fitting of binding kinetics to a four-state reaction mechanism.

The time-dependence of adenine binding to the rA71-U482AP riboswitch was globally fit to the ligand binding mechanism in eq. 1, involving four-states:



in which the k 's are the microscopic rate constants for forward and back reactions.

The changes in the concentration of each RNA state and adenine can be expressed as:

$$d[\text{apo1}]/dt = -k_{\text{op}} [\text{apo1}] + k_{\text{cl}} [\text{apo2}] \quad (2)$$

$$d[\text{apo2}]/dt = k_{\text{op}} [\text{apo1}] - k_{\text{cl}} [\text{apo2}] - k_{\text{on}} [\text{ade}][\text{apo2}] + k_{\text{off}} [\text{IB} \bullet \text{ade}]$$

$$d[\text{ade}]/dt = -k_{\text{on}} [\text{ade}][\text{apo2}] + k_{\text{off}} [\text{IB} \bullet \text{ade}]$$

$$d[\text{IB} \bullet \text{ade}]/dt = k_{\text{on}} [\text{ade}][\text{apo2}] - k_{\text{off}} [\text{IB} \bullet \text{ade}] - k_{\text{f}} [\text{IB} \bullet \text{ade}] + k_{\text{r}} [\text{B} \bullet \text{ade}]$$

$$d[\text{B} \bullet \text{ade}]/dt = k_{\text{f}} [\text{IB} \bullet \text{ade}] - k_{\text{r}} [\text{B} \bullet \text{ade}]$$

The initial concentrations of each species at $t = 0$ are:

$$[\text{apo1}]_0 = k_{\text{cl}} / (k_{\text{op}} + k_{\text{cl}}) C_0;$$

$$[\text{apo2}]_0 = k_{\text{op}} / (k_{\text{op}} + k_{\text{cl}}) C_0;$$

$$[\text{IB} \bullet \text{ade}]_0 = 0;$$

$$[\text{B} \bullet \text{ade}]_0 = 0.$$

The initial concentrations of the closed and open apo conformers are given by the equilibrium $[\text{apo2}]/[\text{apo1}] = k_{\text{op}}/k_{\text{cl}}$. $C_0 = 0.5 \mu\text{M}$ is the total concentration of RNA and $[\text{ade}]_0$ is the initial concentration of adenine in each measurement.

The differential equations in eq. 2 were numerically solved with the initial concentrations above and a given set of rate constants. The change in fluorescence intensity after subtraction of adenine background fluorescence was assumed to reflect the concentration of the bound state, $\text{B}\cdot\text{ade}$, and all of the riboswitch was assumed to have bound ligand after 10 s in $800 \mu\text{M}$ adenine. To compare the calculated trajectories with the experimental data, the concentration of bound riboswitch, $[\text{B}\cdot\text{ade}](t)$, was multiplied by a scalar constant sc , which is equivalent to the relative fluorescence quantum yield. The experimental data sets with various adenine concentrations were globally fit with same scaling value (sc) and rate constants (k 's) by minimizing a Chi-squared error function $Err(k, sc)$ that describes the discrepancy between calculated curves and experimental data sets:

$$Err(k, sc) = \sqrt{\frac{1}{N-1} \sum_{[\text{Ade}]_j} \sum_{\text{time}=i} (\text{Calculated}(i, j) - \text{data}(i, j))^2} \quad (3)$$

The global fitting was performed in MATLAB (MathWorks, MA). To speed up the fitting, the time points were reduced from 5,000 to 120-150 with logarithmic sampling to ensure even weighting of the whole time range.

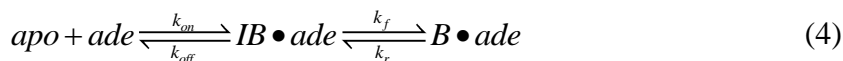
The results of global fitting to eq. 1 are shown in Fig. 2c. Adenine binding ($0.5\text{--}1600 \mu\text{M}$) to $0.5 \mu\text{M}$ rA71-U482AP in 10 mM MgCl_2 at 25°C was measured by stopped-flow spectroscopy of 2AP emission (Extended Data Fig. 4). The kinetic parameters are $k_{\text{op}} = 2.1 \text{ s}^{-1}$, $k_{\text{cl}} = 0.53 \text{ s}^{-1}$, $k_{\text{on}} = 0.37 \mu\text{M}^{-1}\text{s}^{-1}$, $k_{\text{off}} = 45 \text{ s}^{-1}$, $k_{\text{f}} = 132 \text{ s}^{-1}$, $k_{\text{r}} = 5.8 \text{ s}^{-1}$, with $\text{Chi-squared}^{1/2} = 0.025$. When adenine concentration is high, the second-order adenine binding step is faster than conversion of the closed riboswitch to the open riboswitch (k_{op}), resulting in the slower, ligand-

independent phase (0.2 – 10 s) of the reaction (Extended Data Fig.4b). The non-linear rise in the observed rate constant λ_{fast} with respect to adenine concentration results from conversion of the intermediate bound state $IB \bullet ade$ to the final fluorescent bound state $B \bullet ade$ after adenine binds to the apo2 conformer. At high adenine concentration, λ_{fast} approaches the rate of this conformational change (k_f).

The evolution in the concentrations of the four RNA species over time is displayed in Fig. 2d. The concentration of each RNA species was simulated from the kinetic parameters: initial [adenine] = 200 μM , $k_{\text{op}} = 2.1 \text{ s}^{-1}$, $k_{\text{cl}} = 0.53 \text{ s}^{-1}$, $k_{\text{on}} = 0.37 \mu\text{M}^{-1}\text{s}^{-1}$, $k_{\text{off}} = 45 \text{ s}^{-1}$, $k_f = 132 \text{ s}^{-1}$, $k_r = 5.8 \text{ s}^{-1}$, $sc = 2.58$. The fitting error $Err(k, sc) = 0.025$.

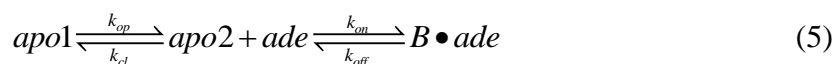
Alternative ligand binding mechanisms

To examine whether two apo forms of the riboswitch are necessary to explain the experimental ligand binding kinetics to rA71-U482AP RNA, we fit the data to a three-state mechanism with only one binding-competent form of the apo riboswitch:



As illustrated in Extended Data Fig. 4d, at least two apo states are necessary to reproduce the observed biphasic ligand binding kinetics. Additional apo states may produce an even closer fit to the binding data in high adenine.

To examine whether the intermediate bound state is needed to accurately describe the experimental binding kinetics, we also attempted to simulate the data with a three-state mechanism lacking the $IB \bullet ade$ intermediate:



In this mechanism, adenine binding to the open form of the riboswitch leads directly to the fluorescent B•ade riboswitch complex. As shown in Extended Data 4e, the intermediate complex is required to reproduce the rate of ligand binding across the entire range of ligand concentrations tested. Therefore, the kinetics of a ligand-induced conformational change at 2AP48 shows that: (1) there is an intermediate bound state (IB•ade) between the initial encounter of ligand with the riboswitch RNA and formation of the final ligand-bound state (B•ade), and (2) there are multiple (two or more) apo states of the riboswitch. These results do not exclude the existence of additional apo or intermediate conformations that may contribute to the operation of the *add* riboswitch.

Reference

- 57 Wickiser, J. K., Cheah, M. T., Breaker, R. R. & Crothers, D. M. The kinetics of ligand binding by an adenine-sensing riboswitch. *Biochemistry* **44**, 13404-13414 (2005).
- 58 Lemay, J. F., Penedo, J. C., Tremblay, R., Lilley, D. M. & Lafontaine, D. A. Folding of the adenine riboswitch. *Chem Biol* **13**, 857-868 (2006).
- 59 Noeske, J., Schwalbe, H. & Wohnert, J. Metal-ion binding and metal-ion induced folding of the adenine-sensing riboswitch aptamer domain. *Nucleic Acids Res* **35**, 5262-5273 (2007).